



## Field line measurements in the divertor of Heliotron-E under boronized conditions

F. Sano<sup>\*</sup>, T. Mizuuchi, T. Hamada, H. Funaba, M. Nakasuga, K. Kondo, H. Zushi, S. Besshou, H. Okada, K. Hanatani, K. Nagasaki, T. Obiki

*Institute of Advanced Energy, Kyoto University, Kyoto, Japan*

---

### Abstract

Vacuum magnetic field line structure of Heliotron-E has been studied experimentally with special reference to the edge plasma physics of the helical system (heliotron/torsatron). A new approach for measuring the vacuum impedance between the magnetic surface and the chamber wall under the boronized conditions was attempted in order to extract the detailed field line topology efficiently. Measurements have revealed the position of the experimental last closed surface and the nesting and folding structure of the divertor field lines. In conclusion, an advanced 2D visualization of Heliotron-E divertor field lines was obtained as compared with the previous one using the stainless-steel wall conditions. In addition, the relationship between the edge plasma distribution and the relevant field line topology is discussed.

*Keywords:* Heliotron-E; Wall coating; Helical divertor; Stochastic boundary; Limiter

---

### 1. Introduction

Since the plasma energy confinement is closely connected with the edge plasma behavior, it is important to study the particle and heat loss mechanisms in the plasma edge with regard to the magnetic field configuration. In the edge region, the field lines in the helical system move stochastically outside the last closed surface. Moreover, there are 'whisker'-like field line structures outside the stochastic region. The separatrix branches in the helical system are sometimes called 'whiskers' which are 'fastened' to a 'whiskered torus' according to Arnold's graphic terminology [1]. Akao [2] studied the edge field line behavior of the heliotron/torsatron type device numerically. He found that three different types of behavior are present, corresponding to three different regions: The stochastic region near the outermost surface, the whisker region, and the inter-whisker region. Based on such a

theoretical prediction, the measurements of the edge magnetic field lines are of essential importance in order to experimentally study the edge plasma loss behavior.

In Heliotron-E divertor operation, the measurements of the ion saturation current in the edge region have been made to investigate such loss behavior, e.g. as shown in Fig. 2(c) of Ref. [3]. It was shown that there were two distinct inflection points of the density gradient ( $X = +26$  cm and  $X = +32$  cm, where  $X$  is the horizontal coordinate.) and that the inflection point of  $X = +32$  cm could be interpreted as being ascribed to the rapid decrease in the connection length of the field line there. However, the explanation of the inflection point at  $X = +26$  cm has not been offered yet. A speculation is that the experimental last closed surface may be present in the neighborhood of  $X = +26$  cm although the calculated position is near  $X = +28.4$  cm. Until now, however, the confident determination of the experimental last closed surface was not easy only by the 1D mapping of the vacuum magnetic surfaces since the magnetic topology of the helical system includes complicated separatrix branches. The motivation of the 2D vacuum magnetic surface mapping was to overcome this difficulty and to obtain the topological

---

<sup>\*</sup> Corresponding author. Tel.: +81-774 383 484; fax: +81-774 329 397; e-mail: sano@ppl.kyoto-u.ac.jp.

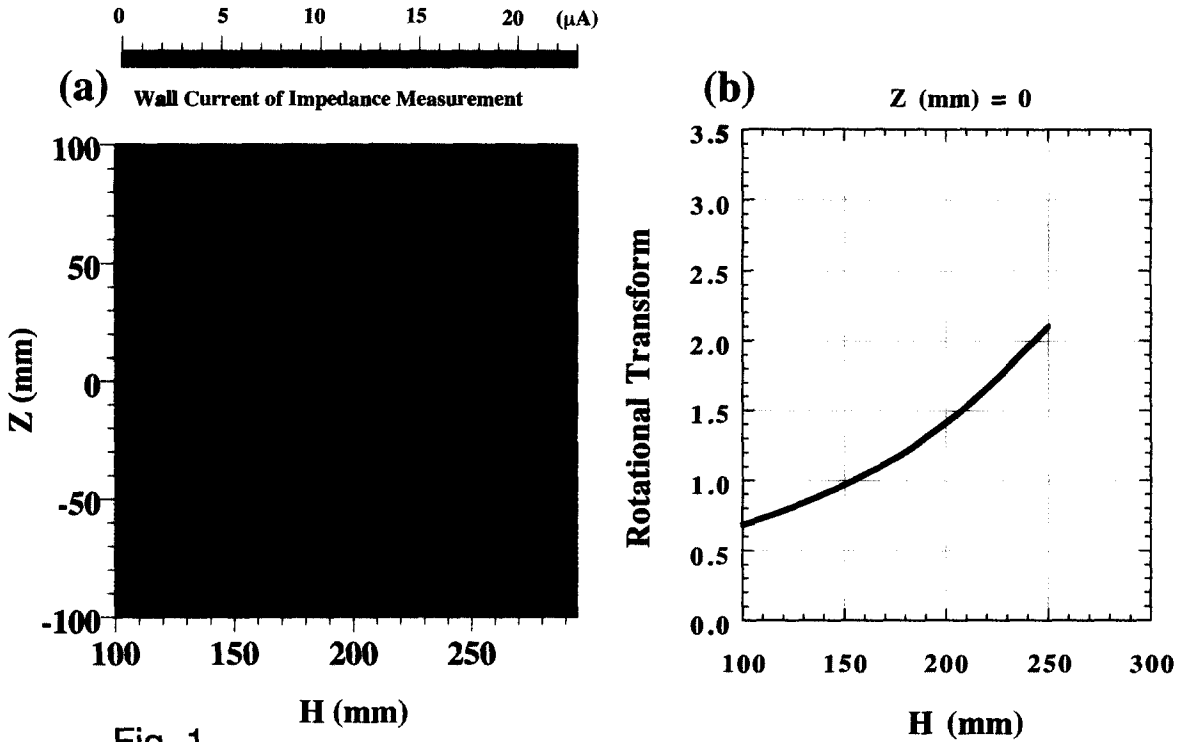


Fig. 1

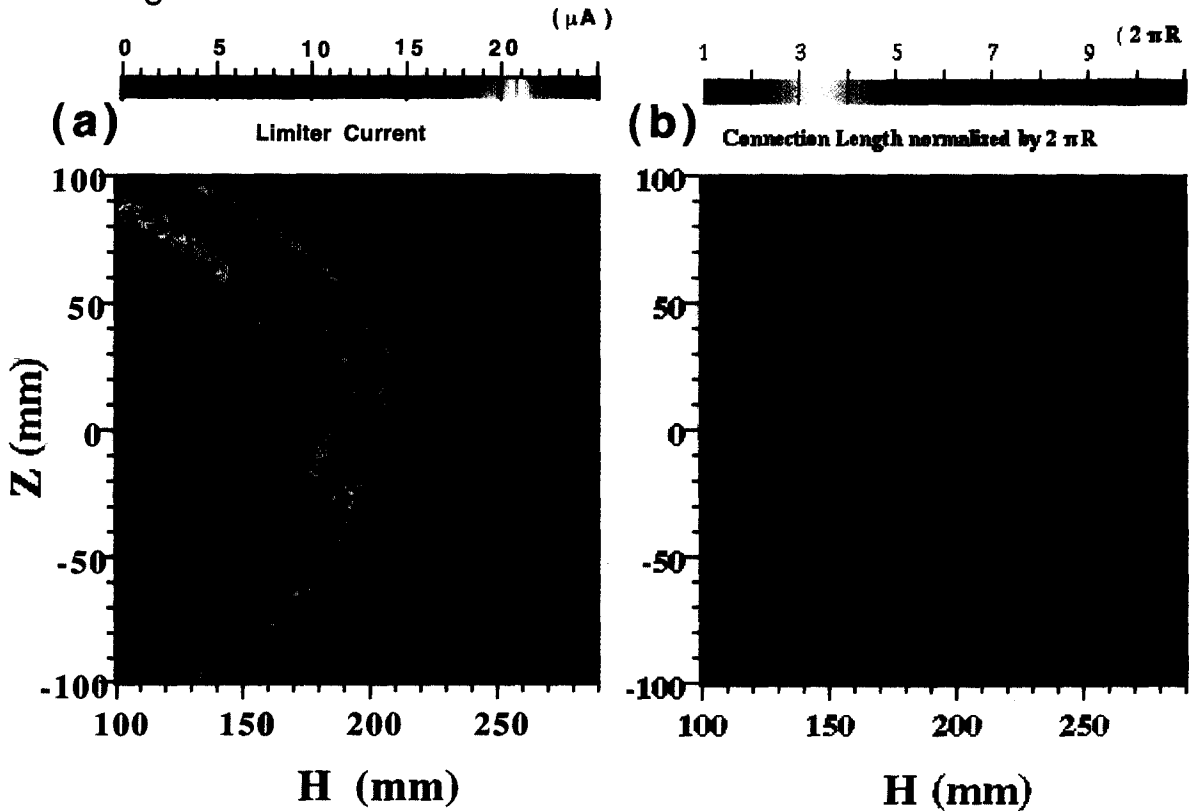


Fig. 2

relationship between the calculated connection length and the experimental wall current of the impedance method.

The impedance method (or ‘stellarator diode method’) developed by Dikii et al. [4] and others [5] is based on the measurement of the emission current from a small hot filament scanned in the vacuum chamber. The original concept was to measure the impedance between the conducting magnetic surface and the chamber wall. The electrons on that surface are diffused toward the wall by electron-neutral collisions. Thus, the electron current flows into the wall, which represents the impedance between the magnetic surface and the chamber wall under the constant bias voltage. We here assume that the surfaces of the constant vacuum impedance coincide with the magnetic (more exactly, with the drift) surfaces. The impedance method has several notable features in comparison with other measurements such as the pulsed-electron-beam method [6] and the luminescent rod method [5]; (i) the impedance method can be applied at weak steady-state magnetic field, so that the measurement is not so time-consuming and (ii) the impedance method can provide quantitative information about the edge and divertor field lines with regard to their connection lengths. Many measurements have been made to confirm the confining magnetic surfaces, but there has been little experimental information about the detailed edge and divertor field line structure in the helical system. The present paper deals with this topic to deepen the understanding of plasma operation.

For Heliotron-E, Takahashi et al. [7] used this technique and thereafter several improvements and modifications of this technique have been introduced in order to pick up the detailed edge topological features. The main characteristics of the present method is (1) to use the 0.5 mm diameter directed electron beam (15 eV) instead of an emissive filament in order to eject the electrons near parallel to the magnetic field lines and (2) to use the boronized wall in order to differentiate the divertor field lines from the wall-to-wall field lines. In the previous method under the stainless-steel wall conditions, the disadvantage was that we could not directly extract the fine-scale

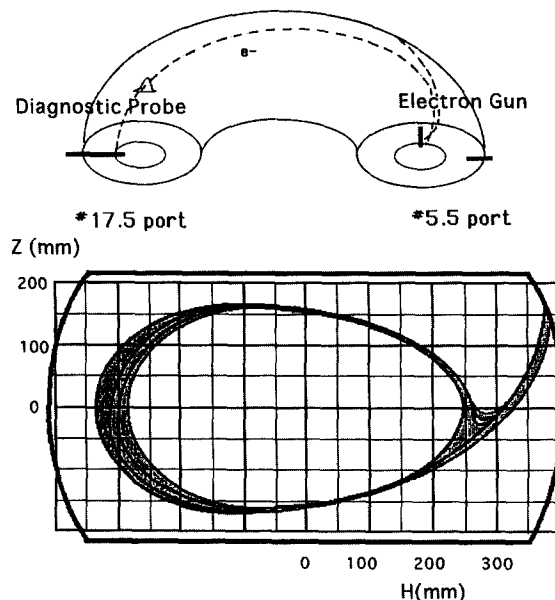


Fig. 3. Schematic of the probe measurement of electron density in the impedance measurement and the notations of the measurement coordinates.

topology. The large detection current through the wall-to-wall field lines could diffuse to the adjacent small-current passages, thus masking the detailed structures. One solution was to apply the Laplacian procedure to the 2D mapping results of the wall current  $I_c(H, Z)$  in order to highlight the dips of the locally small current passages. Here the Laplacian procedure means that we calculate the sum of the second partial derivative of  $I_c(H, Z)$  with respect to  $H$  and the second partial derivative of  $I_c(H, Z)$  with respect to  $Z$ , where  $H$  and  $Z$  are the horizontal and vertical co-ordinates in the poloidal cross section. From this Laplacian procedure, we could identify the narrow whisker field line topology in the fish-mouth zone and in the fish-tail zone for the first time in Heliotron-E. How-

Fig. 1. (a) Contour map of the measured wall current in the impedance measurement under boronized conditions. Under  $B = 500$  G, the 0.5 mm diameter electron beam with 15 eV was ejected near parallel to the magnetic field line at the pressure of about  $2 \times 10^{-8}$  Torr. The measurement of the wall current was performed in the fish-tail zone of the Heliotron-E standard configuration ( $H = 100$  to 300 mm;  $Z = -100$  to 100 mm). (b) Calculated rotational transform for the standard vacuum magnetic configuration of Heliotron-E at the constant vertical position of  $Z = 0$  mm.

Fig. 2. (a) Rings structure of the measured limiter current in the impedance measurement under boronized conditions. Under  $B = 500$  G, the measurement of the limiter current was performed when the carbon limiter was inserted deep in the confinement region of  $Z = -200$  mm in the vertically elongated poloidal cross section of the #6.5 port. The electron gun of the #5.5 port was scanned in the fish-tail zone of the Heliotron-E standard configuration ( $H = 100$  to 300 mm;  $Z = -100$  to 100 mm). (b) Rings structure of the calculated connection length between the electron gun and the limiter. Here the field lines starting from the electron gun can be grouped according to their termination: (A) the confining magnetic surface, (B) the limiter, and (C) the chamber wall. The connection length of group (A) is infinite. To permit ready comparison between the calculated connection length and the measured limiter current, the calculated connection length of group (C) was replaced to be infinite in this figure because the current along the field lines of group (C) does not contribute to the limiter current.

ever, after some experience of this procedure, it was found to be difficult to increase the sensitivity for determining a much finer structure. Therefore, the present paper describes another approach to enhance this sensitivity by utilizing the wall treatment.

## 2. Application of wall boronization to beam impedance method

In order to experimentally discriminate the divertor field lines from that of the wall-to-wall field lines, it is beneficial to differentiate the divertor stripes on the wall from the other wall area by using the boronization. The boronization provides the electrically insulated wall for the

whole inner surface of the chamber. However, the significant localization of plasma-wall interaction on the divertor stripes during some plasma experiments can be utilized to obtain the conducting stripes. Under these conditions, the electron flow on the wall-to-wall field lines can not contribute to the wall-current signal of the impedance method while that on the divertor field lines can contribute to it. Thus the detailed tangling effects of the two groups of field lines can be clearly identified as shown in Fig. 1(a). Obviously, this result is an advanced visualization as compared with the previous 'Poincaré plots image' (obtained using the Laplacian procedure) as shown in Fig. 2(b) of Ref. [8].

On the other hand, the present measurements under the 500 G main magnetic field revealed the existence of the

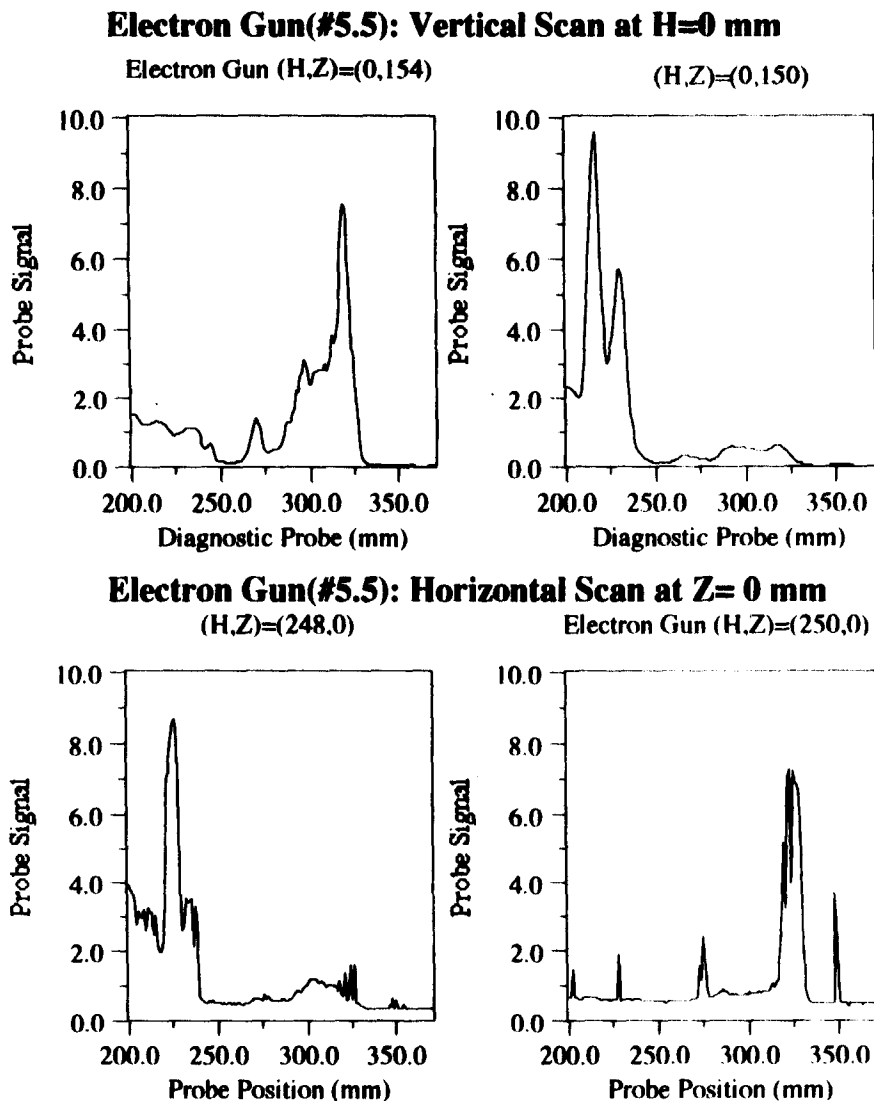


Fig. 4. Measured positions of bifurcation boundary that provides a drastic change of the electron flow.

edge magnetic islands at the positions of  $t = 1.33, 1.67, 2.0$ , etc. as shown in Fig. 1(b). In addition, the primary candidate for the last closed surface was the regular surface at the position of  $t = 2.15$  ( $Z = 0$  mm,  $H = 250$  mm). In order to gain more confidence in this determination, the main magnetic field dependencies of the respective island widths were examined in the 10–500 G operation. The edge islands corresponding to  $t = 1.67$  and  $2.0$  were found to shrink as the main magnetic field is increased. This suggests that the error fields of these islands are non-inductive. An optimistic view is that the extrapolation of this dependence up to  $B = 2$  T indicates the island widths for these islands to become negligible while the position of the last closed surface remains almost unchanged. It is noted that the inner inflection point of the ion saturation current reported previously may be related with this presence of the last closed magnetic surface.

### 3. Connection-length dependence of limiter current

An indicator of the effective connection length averaged over the electron Larmor radius might be obtained from the impedance method. Based on this motivation, we investigated the relationship between the known connection length (between the electron gun and the limiter) and the limiter current when the limiter was inserted deep inside the last closed surface ( $Z = -200$  mm). In this case, the rings structure of the current flowing into the limiter was observed. This finding can be successfully interpreted as being due to the rings structure of the predicted spatial connection-length distribution. Here the field line tracing calculation shows that the connection length between the electron gun (#5.5 port) and the limiter (#6.5 port) is nearly a multiple of the major circumference. Its spatial distribution provides characteristic 2D rings of the discrete rotation numbers. As shown in Fig. 2, the one-rotation band ( $H = 175$  mm at  $Z = 0$  mm) is found to control the last closed surface of the confining region. In addition, several more-than-two-rotation field lines are found to leak inward beyond this band as expected theoretically. This is due to the presence of the  $m = 1/n = 1$  magnetic island which is excited by the earth field in the 500 G main magnetic field operation.

### 4. Probe measurement of electron density in beam impedance method

The local electron density distribution under the conditions of the impedance measurement has been diagnosed with a spherical miniature probe (5 mm diameter) as shown in Fig. 3. The miniature probe inserted at the #17.5 port was scanned horizontally from  $H = 200$  to 350 mm while the electron gun was situated at the #5.5 port (toroidally  $270^\circ$  apart from the probe). The probe measure-

ments clarified the existence of a characteristic boundary across which the spatial electron distribution could change drastically. As shown in Fig. 4, this bifurcation occurs when the electron gun, scanned vertically at the constant horizontal position  $H = 0$  mm, moves from  $Z = 150$  to 154 mm. A reasonable explanation is that when the electron gun is on the separatrix layer, the electron loss is dominated by the parallel loss along the field lines connected with the divertor X-point zone. When the gun is located inside the separatrix layer, the electron density builds up in the central region. The bifurcation boundary is seen to work as a partition between the open field line structure and the closed field line structure. Therefore, this boundary should be recognized as the experimental last closed surface. This position was found to be consistent with that of the previously predicted last closed surface in Section 2. In addition, the similar probe measurement has been made in which the gun at the constant vertical position  $Z = 0$  mm was scanned horizontally from  $H = 200$  to 375 mm. The same bifurcation was observed when the gun was moved from  $H = 248$  to 250 mm. This result was also consistent with what we obtained in the above measurement. The results of Fig. 4 illustrate the experimental behavior of the divertor channel width in the neighborhood of the divertor X-point zone.

### 5. Conclusions

(1) The 2D vacuum geometry of the helical divertor in Heliotron-E was experimentally confirmed at  $B = 500$  G, including a partial destruction of the edge magnetic surfaces. This result could provide an experimental base for studying the edge plasma distribution as well as the relevant plasma loss mechanisms in the high-field plasma operation.

(2) By utilizing the boronized conditions, the proposed impedance method was found to have the distinct advantage in efficiently extracting the divertor field lines over the conventional method.

(3) The present impedance measurement in the limiter insertion mode has revealed that the limiter current is dominated by the connection length between the electron gun and the limiter. This finding supports a model that describes the parallel electron loss (in the limiter shadow) in terms of the connection length.

(4) Under the impedance measurement circumstances, the probe measurements for detecting the electron flow have independently determined the position of the experimental last closed surface. This position was consistent with that of the above impedance measurement and was found to be located a few cm inside ( $X = +25$  cm) with regard to the numerically predicted position ( $X = +28.4$  cm).

(5) A possibility was presented that the existence of the inner inflection point of the edge density gradient which

was reported previously could be ascribed to the experimental last closed magnetic surface.

(6) Because of its good performance, the present technique will allow its application to the divertor field line measurements of much larger helical systems such as LHD in Japan and WVII-X in Germany.

#### Acknowledgements

We are grateful to the members of the Heliotron-E operation group for their assistance in the measurements.

#### References

- [1] B.V. Chirikov, Phys. Rep. 52 (1979) 263.
- [2] H. Akao, J. Phys. Soc. Jpn. 59 (1990) 1633.
- [3] H. Matsuura et al., Nucl. Fusion 32 (1992) 405.
- [4] A.G. Dikii et al., Sov. J. Plasma Phys. 14 (1988) 160.
- [5] G.G. Lesnyakov et al., Nucl. Fusion 32 (1992) 2157.
- [6] T. Mizuuchi, S. Morimoto, A. Iiyoshi and K. Uo, Nucl. Fusion 22 (1982) 247.
- [7] R. Takahashi et al., Jpn. J. Appl. Phys. 28 (1989) 2604.
- [8] F. Sano et al., Trans. Fusion Technol. 27 (1995) 206.